


---

This is the **accepted version** of the journal article:

Rodriguez, Sady Roberto; Guillén, Marina; Romero, Oscar. «Enhancing Multi-Enzymatic CO<sub>2</sub> Conversion via Reactor Engineering : Effects of Mass Transfer on Sustainable and Green Metrics». *Green chemistry*, DOI 10.1039/D6GC00387G

---

This version is available at <https://ddd.uab.cat/record/327349>

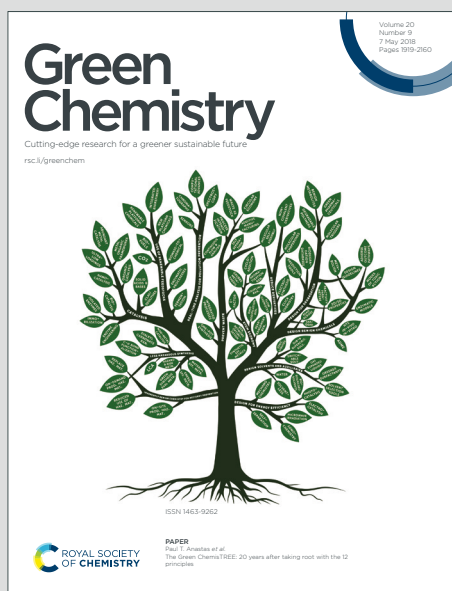
under the terms of the  license.

# Green Chemistry

Cutting-edge research for a greener sustainable future

Accepted Manuscript

This article can be cited before page numbers have been issued, to do this please use: S. R. Rodriguez, M. Guillén and O. Romero, *Green Chem.*, 2026, DOI: 10.1039/D6GC00387G.



This is an Accepted Manuscript, which has been through the Royal Society of Chemistry peer review process and has been accepted for publication.

Accepted Manuscripts are published online shortly after acceptance, before technical editing, formatting and proof reading. Using this free service, authors can make their results available to the community, in citable form, before we publish the edited article. We will replace this Accepted Manuscript with the edited and formatted Advance Article as soon as it is available.

You can find more information about Accepted Manuscripts in the [Information for Authors](#).

Please note that technical editing may introduce minor changes to the text and/or graphics, which may alter content. The journal's standard [Terms & Conditions](#) and the [Ethical guidelines](#) still apply. In no event shall the Royal Society of Chemistry be held responsible for any errors or omissions in this Accepted Manuscript or any consequences arising from the use of any information it contains.

## Green Foundation Box

View Article Online  
DOI: 10.1039/D6GC00387G

1. This work advances green chemistry as the first enzymatic Carbon Capture and Utilization (CCU) report using environmental metrics to support carbon-neutral manufacturing. It valorises industrial emissions and renewable feedstocks into high-value chemicals, significantly reducing the environmental footprint for climate change.
2. The system achieved a record 66.1 mM formate production, 93.3% capture efficiency, and complete conversion into high-value products. This achievement demonstrates high process selectivity and a remarkably low Global Warming Potential (GWP) of 13.2 kg CO<sub>2</sub> eq per kg of product.
3. Future work should focus on: 1) optimizing FDH catalytic efficiency ( $k_{\text{cat}}/K_{\text{m}}$ ) via protein engineering or bioprospecting to overcome kinetic bottlenecks, and 2) enhancing CO<sub>2</sub> mass transfer through synergy with Carbonic Anhydrase (CA).



# Enhancing Multi-Enzymatic CO<sub>2</sub> Conversion via Reactor Engineering: Effects of Mass Transfer on Sustainable and Green Metrics

View Article Online  
DOI: 10.1039/D6GC00387G

*Sady Roberto Rodriguez, Marina Guillén & Oscar Romero\**

Bioprocess Engineering and Applied Biocatalysis Group, Department of Chemical,  
Biological and Environmental Engineering, Universitat Autònoma de Barcelona, 08193  
Bellaterra, Spain.

## Corresponding Author

**\*Oscar Romero Ormazábal**

Department of Chemical, Biological and Environmental Engineering, Universitat  
Autònoma de Barcelona, 08193 Bellaterra, Catalonia, Spain.

[Oscar.Romero.Ormazabal@uab.cat](mailto:Oscar.Romero.Ormazabal@uab.cat)



## Abstract

The global energy transition toward decarbonization requires highly efficient Carbon Capture and Utilization (CCU) technologies that combine economic feasibility, operational stability and environmental sustainability. A key factor for successful CCU is efficient CO<sub>2</sub> gas–liquid transfer, which can be optimized through tailored reactor designs to maximize yields and utilization. Technological advances such as CO<sub>2</sub>-specific sensors have enabled accurate monitoring of CO<sub>2</sub> mass balance enhancing the efficiency of its conversion. This work addresses an in-depth analysis of CO<sub>2</sub> mass transfer in a stirred-tank reactor, focusing on the impact of volumetric gas flow rate on gas-liquid transfer during the multi-enzymatic conversion of CO<sub>2</sub> into high-value compounds using a co-immobilized biocatalyst of formate dehydrogenase and glycerol dehydrogenase enzymes. The volumetric mass transfer coefficient ( $k_La$ ) was determined at different gas flow rates (1, 0.5 and 0.1 vvm) from a 24% CO<sub>2</sub> gas mixture, with the reaction carried out at 0.1 vvm achieving an outstanding formate production of  $66.1 \pm 1.4$  mM ( $3 \text{ g L}^{-1}$ ), due to near-neutral pH conditions that improved the reaction conditions and enhanced biocatalyst stability by at least 1.8-fold compared with high gas flow rate (1.0 vvm). Furthermore, a remarkable CO<sub>2</sub> capture efficiency of  $93.3 \pm 2.1\%$  was achieved at 0.1 vvm, along with a high selectivity toward formate and glycerol carbonate, reflecting a complete CO<sub>2</sub> conversion into target products. Finally, the environmental impact of the reaction at 0.1 vvm showed a lower contribution to climate change, reaching  $13.2 \text{ kg CO}_2 \text{ eq kg products}^{-1}$ . These results underscore enzymatic CO<sub>2</sub> reduction as an effective and sustainable approach for the development of bio-based industrial processes with a markedly reduced environmental footprint.



**Keywords:** CO<sub>2</sub> capture, Enzymatic reduction, Reactor engineering, Gas-liquid transfer, Global Warning Potential.

[View Article Online](#)  
DOI: 10.1039/D6GC00387G

Global Warning Potential.

## 1. INTRODUCTION

Carbon dioxide (CO<sub>2</sub>) is gaining increasing recognition as a valuable carbon feedstock as the global energy landscape shifts toward decarbonization. In this context, CO<sub>2</sub> conversion technologies offer a strategic approach to simultaneously enhance energy storage, contribute to global climate objectives, and promote the development of a circular carbon economy. (1) However, scaling up these technologies to industrial processing plants requires comprehensive optimization to ensure economic viability and operational stability. (2) Despite significant advances to develop more efficient catalysts for CO<sub>2</sub> reduction and translating these processes to larger scales, studies focusing on reactor engineering aspects to optimize these catalytic processes remain limited. (3)

For conventional chemical reactions, including catalytic conversions, reactor engineering has long provided a robust and effective framework for achieving maximum productivity while minimizing cost and energy losses. (4) Moreover, this approach is crucial for enhancing reaction performance, facilitating efficient mass and heat transfer, improving product selectivity and increasing overall process efficiency. (4,5) Under these principles, a fundamental requirement for the success of both CO<sub>2</sub> capture and utilization processes is the efficient transfer from the gas to the aqueous phase, enabling effective mitigation. (6) Therefore, evaluating CO<sub>2</sub> mass transfer through tailored reactor configurations is essential to advance industrial deployment of CCU technologies.



Under this context, the volumetric mass transfer coefficient ( $k_L a$ ) is a key parameter that quantifies the rate of gas movement to the liquid phase, directly influencing reaction kinetics and overall performance in inter-phase systems.  $k_L a$  is commonly used to assess reactor efficiency, optimize the design and operation of mixing and sparging equipment, and plays a critical role in process scale-up. (7) In many processes involving the direct conversion of gases such as CO<sub>2</sub> or oxygen (O<sub>2</sub>), mass transfer may be slower than the reaction rate; therefore, the rate of gas - liquid transfer becomes the limiting step of the entire process, and its optimization is therefore crucial. (8) Furthermore, in the case of CO<sub>2</sub> there is an additional step during this transfer, the chemical reaction rate at which CO<sub>2</sub> reacts with water to form various inorganic carbonate species in equilibrium. (9) Therefore, assessing the volumetric mass transfer coefficient of CO<sub>2</sub> in the biocatalytic reaction is crucial for evaluating reaction rates, improving process efficiency, optimizing reactor performance and enabling successful scale-up.

CO<sub>2</sub> gas – liquid transfer has been typically considered as analogous to O<sub>2</sub> transfer by applying correction factors to account for differences in diffusion coefficients between the two gases. (10) This approach stems from the extensive availability of O<sub>2</sub> sensors, the ease of measuring O<sub>2</sub> transfer, and the abundance of published data. (11) However, modern advances have enabled the development of CO<sub>2</sub>-specific sensors that directly measure gas–liquid transfer by detecting pH changes caused by inorganic carbon species (7) , as the digital in-line CO<sub>2</sub> sensor used in this work. In addition, most CO<sub>2</sub> mass-transfer studies have focused on low pH conditions, where its equilibrium concentration is higher, while only few have evaluated its  $k_L a$  at neutral or higher pH. (12)



Consequently, by applying mass transfer analysis and reactor engineering principles, it is possible to integrate instrumentation such as sensors and control systems that generate reliable data to evaluate the overall process balance, ensuring favorable economics when all reactor components perform optimally. Furthermore, adjusting the gas supply rate to maintain the dissolved CO<sub>2</sub> concentration near the optimum for the reaction conditions can reduce unnecessary gas expenditure and maximize the fraction effectively converted into product. (13)

In this study, we investigate the mass transfer of CO<sub>2</sub> in a multi-enzymatic reduction system for the simultaneous production of three high value-added compounds: formate, dihydroxyacetone (DHA) and glycerol carbonate (GC) (Fig. 1). In our previous work, the multi-enzymatic system was developed using the enzymes formate dehydrogenase (FDH) and glycerol dehydrogenase (GlyDH) in their free form (14), as well as co-immobilized on the Ni<sup>2+</sup>-ReliZyme carrier (bifunctional biocatalyst) (15). FDH enzyme has been considered a key model for the design of CO<sub>2</sub> fixation systems, enabling the production of the only CO<sub>2</sub>-derived product currently manufactured at industrial scale, formic acid or formate. (16) This compound finds a wide range of industrial applications, serving as a chemical feedstock, in the textile and leather industries, and as a food additive. (17) To complement this reaction, GlyDH was selected to enable *in situ* cofactor regeneration through glycerol valorization, which is abundantly generated as a byproduct of the biodiesel industry, making it an industrially relevant and low-cost feedstock. (18) From this, DHA is produced, a compound utilized as a tanning agent in the cosmetic industry and as a building block in pharmaceutical synthesis. (19) This FDH–GlyDH synergy has



ensured efficient NADH cofactor recycling while simultaneously coupling two thermodynamically challenging reactions and adding value to industrial feedstocks like CO<sub>2</sub> and glycerol. (14) .Additionally, GC is formed as a byproduct through the direct carboxylation of CO<sub>2</sub> and glycerol (20) [reaction mechanism in Fig S2, SI], catalyzed by metals such as nickel (Ni<sup>2+</sup>) on the immobilization carrier and zinc (Zn<sup>2+</sup>) in the active site of metalloenzyme GlyDH from *Bacillus stearothermophilus*. (21). This is another high-value chemical with applications in the polymer, pharmaceutical, and cosmetic industries, as well as a versatile intermediate in green chemistry and sustainable synthesis. (20)

For this work, through reactor engineering, the setup of the multi-enzymatic reaction enabled the development of a mass balance to quantify CO<sub>2</sub> captured and converted at different gas flow rates using an *in situ* sensor system. Likewise, the environmental impact of this bioprocess was assessed through its contribution to climate change (GWP: Global Warming Potential). These findings represent a novelty in the study of CO<sub>2</sub> mass transfer in biocatalytic processes and provide a framework to support the development of sustainable and environmentally friendly systems that combine the capture of CO<sub>2</sub> gas emissions and their subsequent conversion into valuable compounds in a single step.

View Article Online  
DOI: 10.1039/D6GC00387G



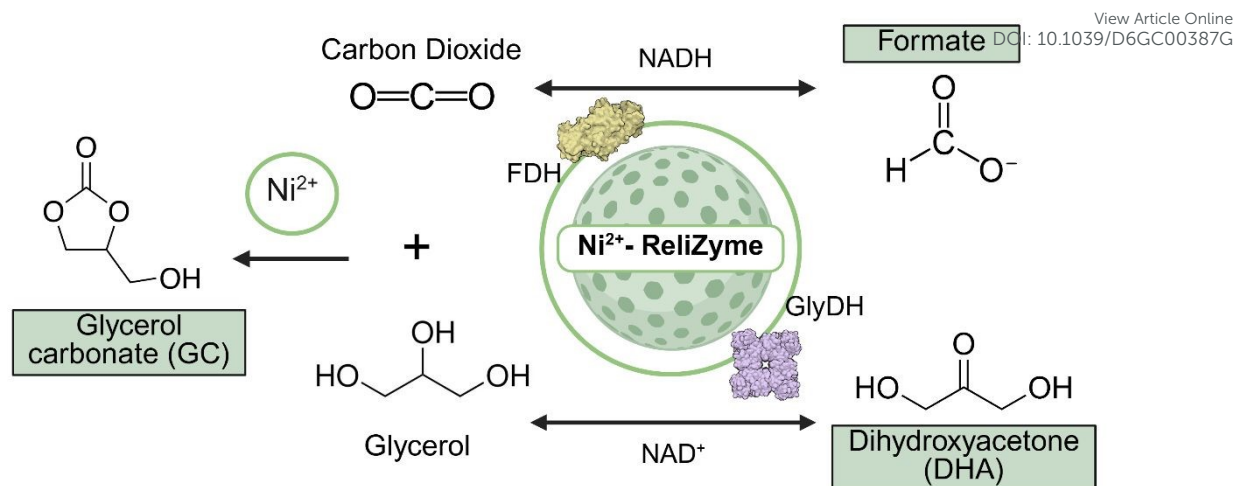


**Figure 1.** Overview of the multi-enzymatic system for CO<sub>2</sub> reduction to high-value compounds. The co-production of formate and DHA - from CO<sub>2</sub> and glycerol - is enzymatically catalyzed by formate dehydrogenase (FDH) and glycerol dehydrogenase (GlyDH) enzymes co-immobilized on the Ni<sup>2+</sup>-ReliZyme carrier, allowing the *in situ* NADH regeneration. Likewise, the synthesis of the by-product glycerol carbonate (GC) from CO<sub>2</sub> and glycerol is catalyzed by the nickel (Ni<sup>2+</sup>) present in the bifunctional biocatalyst (prepared on Ni<sup>2+</sup>-ReliZyme carrier) and zinc (Zn<sup>2+</sup>) in the active site of GlyDH from *Bacillus stearothermophilus*.

## 2. EXPERIMENTAL

### 2.1. Materials

All reagents were purchased from Sigma Aldrich® (St. Louis, MO, USA) and PanReac Quimica S.L.U. (Barcelona, Spain). The cofactors NADH and NAD<sup>+</sup> were purchased from GERBU Biotechnik GmbH (Heidelberg, Germany). ReliZyme™ EP403S resin was purchased from Resindion S.r.l. (Binasco, Italy). All samples and buffers were prepared in Milli Q water (18.2 MΩ cm, Merck Millipore, USA). The gas mixture 24% CO<sub>2</sub> and 76% N<sub>2</sub> was obtained from Carburos Metalicos (Barcelona, Spain). Formate



dehydrogenase (EC 1.17.1.9) and Glycerol dehydrogenase (EC 1.1.1.6) enzymes were produced and purified by the research group according to the procedures reported by the authors. (14)

## 2.2. Determination of the CO<sub>2</sub> volumetric mass transfer coefficient ( $k_L a$ )

The volumetric mass transfer coefficient ( $k_L a$ ) for CO<sub>2</sub> was determined in a stirred-tank reactor (SpinChem, Sweden) with 200 mL of phosphate buffer 100 mM (pH 7.5) as reaction medium, temperature of 30°C and stirring set at 300 rpm. A gas mixture composed of 24% CO<sub>2</sub> in nitrogen, similar to the off-gases composition from blast furnaces in the iron and steel industry (24.5% CO<sub>2</sub>) (22) was employed. The dissolved CO<sub>2</sub> concentration was monitored using a digital in-line CO<sub>2</sub> sensor InPro5000i/12/220 (Mettler Toledo S.A.E., Barcelona, Spain). This sensor was immersed in the liquid at the same depth for all experiments and the data was collected by an Analytical Transmitter M400 Type 3 (Mettler Toledo S.A.E., Barcelona, Spain). The volumetric gas flow rate per volume of liquid per minute (vvm) was assessed at 0.1, 0.5, 1.0, and 1.5 vvm. Additionally, the effect of the immobilization carrier (Ni<sup>2+</sup>-ReliZyme) resuspended in the medium was evaluated by applying loadings of 5%, 10%, 15%, and 20% of the total reaction volume. Sensor response time was assessed by equilibrating the CO<sub>2</sub> concentration in the medium and then transferring the sensor to a CO<sub>2</sub>-free medium, according to the equation in section S5 in the Supplementary Information (SI). The  $k_L a$  was calculated using the following equation, applying a nonlinear model with the Solver tool (Microsoft ® Excel):

$$C_{\text{mes}} = C^* + \frac{C^* - C_0}{1 - \tau k_L a} \left[ \tau k_L a \exp\left(-\frac{t}{\tau}\right) - \exp(-k_L a t) \right] \text{ (Eq. 1)}$$

Where:



$C_{\text{mes}}$ : CO<sub>2</sub> concentration measured by the sensor at certain time  $t$

View Article Online  
DOI: 10.1039/D6GC00387G

$C^*$ : Equilibrium or saturation CO<sub>2</sub> concentration in the liquid phase

$C_0$ : Initial dissolved CO<sub>2</sub> concentration in the medium.

$k_L a$ : The volumetric mass transfer coefficient (min<sup>-1</sup>)

$\tau$ : Sensor response time

$t$ : Time at which the CO<sub>2</sub> concentration is measured

### 2.3. Multi-enzymatic reduction of CO<sub>2</sub> by assessing different volumetric gas flow rates

The multi-enzymatic reduction of CO<sub>2</sub> was performed in a stirred-tank reactor using a co-immobilized bifunctional biocatalyst, with *in situ* NADH regeneration and continuous gas supply. As reaction medium, phosphate buffer 100 mM (pH 7.5) was used with NADH 1 mM, glycerol 100 mM, and gas continuously bubbled at volumetric flow rates of 0.1, 0.5, and 1 vvm from a gas mixture with 24% CO<sub>2</sub> in nitrogen, using a mass flow controller EL-FLOW (Bronkhorst, Netherlands). A total of 20 g of biocatalyst (containing approximately 40 mg g<sup>-1</sup> of GlyDH and 10 mg g<sup>-1</sup> FDH) were suspended in 200 mL of reaction medium. The preparation of this biocatalyst is detailed in Supplementary Information (Section S1).

To monitor the CO<sub>2</sub> inlet and outlet of the reactor, two BCP-CO<sub>2</sub> gas analyzers were installed for *in situ* CO<sub>2</sub> measurements (measured every 5 min). The data were collected and analyzed using the BlueVis software. (BlueSens GmbH, Germany). A digital in-line CO<sub>2</sub> sensor InPro5000i/12/220 was also incorporated to measure its dissolved concentration (measured every 2 min) and the data was collected by an Analytical Transmitter M400 Type 3 (Mettler Toledo S.A.E., Barcelona, Spain). Additionally, a Syntrode pH electrode, connected to a 916 Ti-Touch titrator (Metrohm Hispania, S.L.U, Spain), was installed to continuously monitor the pH throughout the reaction, measuring



every hour. Figure 2 shows the full flow diagram of the reaction setup with the sensors involved. The experiments were conducted in duplicate at 30°C with constant stirring at 300 rpm over 80 h. Samples were taken periodically to analyze substrate and product concentrations, as well as enzyme activity (Sections S2 and S4, SI).

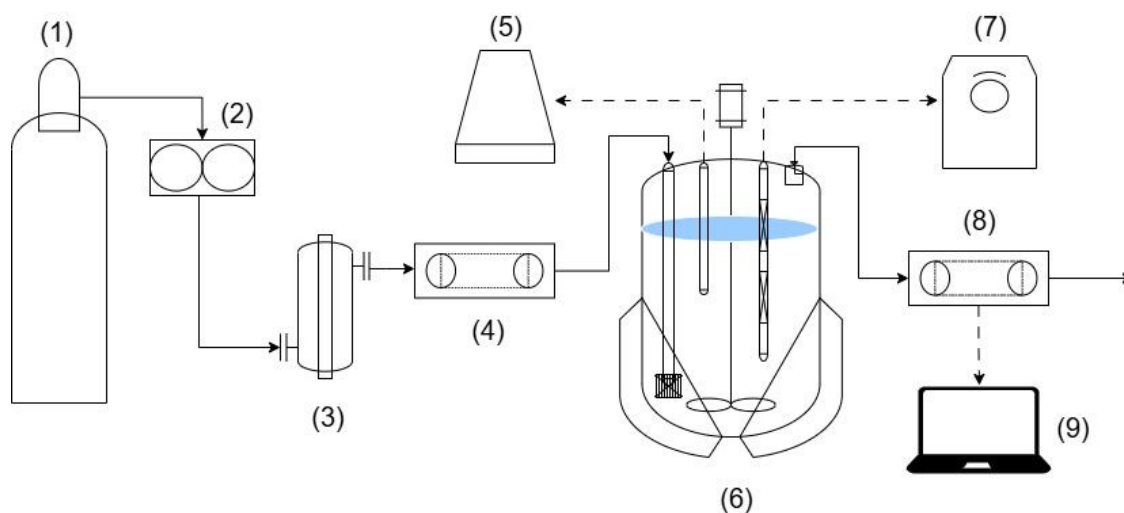


**Figure 2.** Flow diagram of the setup for the multi-enzymatic reduction of CO<sub>2</sub> to high value chemicals. (1) Gas mixture 24% CO<sub>2</sub> in N<sub>2</sub>. (2) Gas flowmeter. (3) Gas humidification. (4) CO<sub>2</sub> input sensor. (5) pH-monitoring titrator. (6) Stirred-tank reactor. (7) Dissolved CO<sub>2</sub> analytical transmitter. (8) CO<sub>2</sub> output sensor. (9) Gas sensor data collection and analysis. (—) Continuous gas flow. (---) Data collection.

#### 2.4. CO<sub>2</sub> mass balance analysis

The mass balance of CO<sub>2</sub> during the reaction was determined through the sensor-based system integrated into the experimental setup previously detailed. First, the amount of CO<sub>2</sub> at the inlet and outlet of the reactor per unit of time (h) was calculated following Equations S2 and S3. Accordingly, the mass of CO<sub>2</sub> captured was calculated using the following equation:



$$\text{CO}_2 \text{ captured (g h}^{-1}\text{)} = \text{CO}_2 \text{ inlet (g h}^{-1}\text{)} - \text{CO}_2 \text{ outlet (g h}^{-1}\text{)} \quad (\text{Eq. 2})$$

Afterwards, the total amount of CO<sub>2</sub> (in g) that entered the reactor and the amount captured throughout the reaction were calculated by estimating the area under the curve according to equation S4 in SI.

For CO<sub>2</sub> converted to formate and glycerol carbonate (GC), only the fraction of CO<sub>2</sub> atoms incorporated into each product was considered. As reported by Gao *et al.* (23), all CO<sub>2</sub> atoms participate in forming the linear carbonate intermediate during glycerol carbonate synthesis, as well as in formate synthesis. Therefore, correction factors were calculated based on the molecular weights of CO<sub>2</sub> and each product, as described by Equation S5 in SI. These factors were then incorporated into the subsequent equation to determine the mass of CO<sub>2</sub> converted into product:

$$\text{CO}_2 \text{ converted (g)} = \text{Amount of product (g)} \times \text{CF} \quad (\text{Eq. 3})$$

Where:

CF formate= 0.978

CF glycerol carbonate = 0.373

The total amount of CO<sub>2</sub> converted corresponds to the sum of the CO<sub>2</sub> incorporated into each product.



The product yields obtained per g of CO<sub>2</sub> captured were calculated based on the total mass of each molecule produced and expressed as g g<sup>-1</sup> (dimensionless). The following equation was employed:

$$\text{Product yield (g g}^{-1}\text{)} = \frac{\text{Total mass of formate or GC produced (g)}}{\text{Mass of CO}_2\text{ captured (g)}} \quad (\text{Eq. 4})$$

Finally, two CO<sub>2</sub> conversion performance metrics commonly employed in the green chemistry were considered. First, process selectivity refers to the system's ability to direct captured CO<sub>2</sub> toward the desired product, reflecting the reaction efficiency under the given conditions. The following equation was applied:

$$\text{Selectivity (\%)} = \frac{\text{moles product (formate or GC)}}{\text{moles CO}_2\text{ captured}} \times 100 \quad (\text{Eq. 5})$$

The sum of the selectivity toward each product represents the global process selectivity.

On the other hand, carbon efficiency indicates how effectively carbon introduced into a process is incorporated into the final product, accounting indirectly for losses in by-products or emissions and providing a key measure of process sustainability and economic efficiency. The carbon efficiency equation used in this work was adapted from Belsa *et al.* (24) and Constable *et al.* (25), indicating the sum of the yields of the final CO<sub>2</sub>-derived products, formate and glycerol carbonate (GC):

$$(\text{Eq. 6})$$



$$\text{Carbon efficiency} = \frac{\sum C_x n_x}{n_{\text{CO}_2}} \times 100$$

View Article Online  
DOI: 10.1039/D6GC00387G

Where

$C_x$  = number of carbons from  $\text{CO}_2$  in each product  $x$  (one single carbon)

$n_x$  = number of moles of each product (formate or GC)

$n_{\text{CO}_2}$  = number of moles of  $\text{CO}_2$  that entered the system

## 2.5. Environmental impact assessment

To assess the environmental impact of this process on climate change, the global warming potential (GWP) was determined for each reaction performed at different volumetric flow rates. The GWP was calculated based on the product mass (Eq. 7) and the energy consumed (Eq. 8), following the equations proposed by Domínguez de María (26) :

$$\text{GWP} \left( \text{water} \left( \text{wwtp} \right) \right) = \frac{0.073 \times \% \text{water treated}}{\text{conv.} \times [\text{SL}]} \quad (\text{Eq. 7})$$

$$\text{GWP} \left( \text{water} \left( \text{energy} \right) \right) = \left( \frac{0.037 \times \Delta T}{\text{conv.} \times [\text{SL}]} \right) + t \left( \frac{0.0056 \times \Delta T}{\text{conv.} \times [\text{SL}]} \right) \quad (\text{Eq. 8})$$

Where:

wwtp = wastewater treatment plant

conv.:  $\text{CO}_2$  conversion (%)

[SL]: Product concentration expressed in  $\text{kg L}^{-1}$ .

$t$ : Reaction time (80 h)



Considerations: 100% of the residual water was assumed to be treated in a WWTP Room

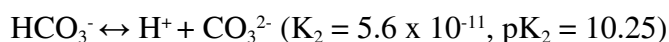
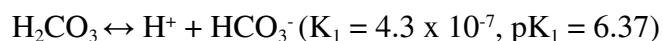
View Article Online  
DOI: 10.1039/D6GC00387G

temperature was set at 25 °C.

### 3. RESULTS AND DISCUSSION

#### 3.1. Determination of the volumetric mass transfer coefficient ( $k_L a$ ) of CO<sub>2</sub> in a stirred-tank reactor

To study CO<sub>2</sub> mass transfer, its volumetric mass transfer coefficient ( $k_L a$ ) was determined in the stirred-tank reactor used for the multi-enzymatic CO<sub>2</sub> reduction reaction. Estimating  $k_L a$  for CO<sub>2</sub> is crucial in bioreactor design, as it assesses reactor efficiency and guides scale-up, especially in processes requiring continuous CO<sub>2</sub> supply, such as in several chemical processes and in some fermentations. (27) Moreover, optimizing CO<sub>2</sub> transfer also reduces costs by supplying only the necessary gas amount, thereby improving resource efficiency. (28) However, understanding CO<sub>2</sub> chemical equilibrium in water is essential to evaluate its mass transfer in aqueous systems. CO<sub>2</sub> interacts with water to form carbonic acid, bicarbonate, and carbonate, following this dissociation equilibria at pH 7.0 and 30 °C (29) :



According to some reports, the Total Inorganic Carbon (TIC), which reflects the distribution of these species as a function of the medium's pH, is a key parameter for studying CO<sub>2</sub> gas-liquid transfer, since it not only estimates the amount of CO<sub>2</sub> absorbed



but also identifies the dominant form in which it is present. (12) This parameter can be determined using conventional methods such as alkalinity titration or specialized techniques like Non-Dispersive Infrared (NDIR) analysis. (30) However, in this study,  $k_L a_{(CO_2)}$  was determined using a dynamic method that requires continuous real-time tracking of the dissolved  $CO_2$  concentration. For that, a digital in-line  $CO_2$  sensor was employed, which measures only dissolved  $CO_2$  ( $mg\ L^{-1}$ ). This provides a simplified methodology and enables immediate *in situ* tracking of concentration changes, which are essential for the accurate and rapid determination of  $k_L a$  throughout the process. The operating principle of this sensor, based on the Severinghaus principle, is illustrated in Figure S1 in SI.

In general,  $k_L a$  determination depends on reactor type and volume, operating conditions (temperature, pH, pressure, agitation), flow rate, immersion depth, suspended solids and the properties of the gas and liquid phases, among other factors. (31) In this work, the agitation speed was set at 300 rpm to prevent biocatalyst damage at higher stirring rates. Consequently, other factors such as gas flow rate and resuspended solids (immobilization carrier), were examined. As an initial step, the response time of the dissolved  $CO_2$  sensor ( $\tau$ ) was assessed according to equation S1 in SI. Figure S3 in the SI provides a graphical illustration and a brief discussion of the sensor's response to a  $CO_2$ -free medium, yielding a response time of 0.93 min (56 s).



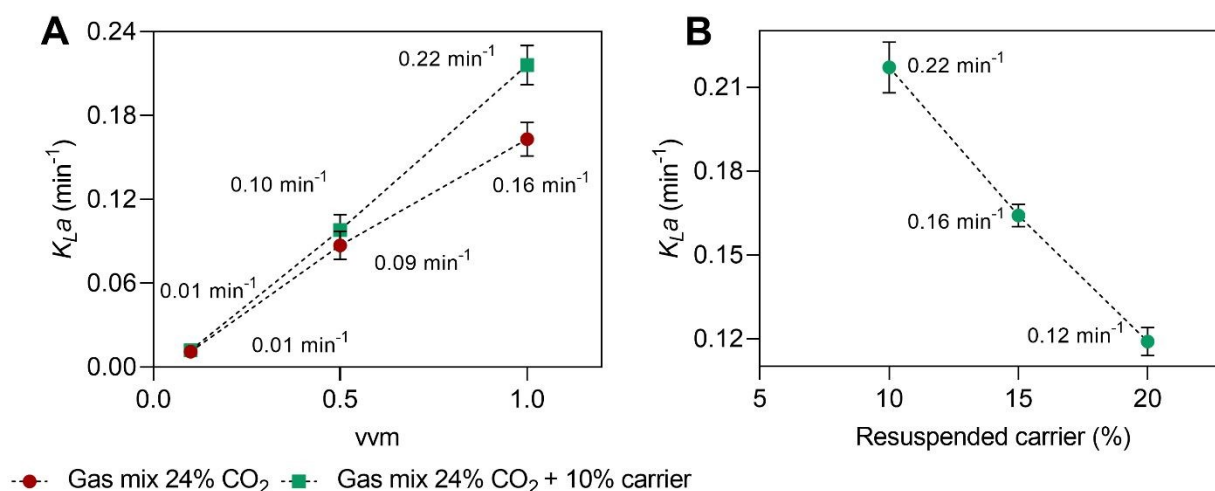
Figure 3 shows the  $k_L a_{(\text{CO}_2)}$  values obtained by evaluating different volumetric flow rates of the 24%  $\text{CO}_2$  mixture, along with the immobilization carrier ( $\text{Ni}^{2+}$  - ReliZyme) present at 10% of the total volume are plot. As expected, the  $\text{CO}_2$  gas–liquid transfer rate increased with the volumetric flow rate from 0.1 to 1 vvm, while no further increase was observed at 1.5 vvm, indicating that the mass transfer limit had been reached (Fig. 3A). In experiments with 10% resuspended carrier,  $k_L a_{(\text{CO}_2)}$  increased compared to assays without carrier, particularly at higher flow rates such as 1 vvm (Fig. 3A). Suspended solids likely enhance gas–liquid transfer by increasing turbulence and dispersing gas bubbles, expanding the surface area for solubilization. (32) As before, no further increase was observed at 1.5 vvm.

Table S1 in the SI summarizes the parameters evaluated for  $k_L a_{(\text{CO}_2)}$  in the experiments described. Across flow rates from 0.1 to 1 vvm, the data were well described by a linear model ( $R^2 > 0.99$ ). Under these conditions, a  $\text{CO}_2$  gas–liquid transfer rate of  $7.35 \pm 0.44 \text{ mg L}^{-1} \text{ min}^{-1}$  ( $0.17 \pm 0.02 \text{ mM min}^{-1}$ ) was achieved with 10% resuspended carrier at 1 vvm. The  $k_L a_{(\text{CO}_2)}$  was also determined with pure  $\text{CO}_2$ . As expected, a highest transfer rate was observed, yielding a  $k_L a$  of  $0.32 \pm 0.03 \text{ min}^{-1}$  ( $10.75 \text{ mg L}^{-1} \text{ min}^{-1}$ , Table S1), due to the higher partial pressure driving faster gas–liquid transfer.

Finally, varying the resuspended carrier at 1 vvm (Fig. 3B) showed that concentrations above 10% caused a linear decrease in  $k_L a_{(\text{CO}_2)}$ , likely due to interface saturation and increased fluid viscosity limiting bubble mobility. (33) Minimal differences were observed between 5% and 10%, suggesting a negligible effect within this range. Hence,



a carrier concentration in that range (from 10 – 20%) and volumetric flow rate from 0.1 – 1.0 vvm from the gas mixture 24% CO<sub>2</sub> may represent the optimal operating conditions for this multi-enzyme system.



**Figure 3.** (A) Gas-liquid CO<sub>2</sub> transfer rate ( $k_{La}$ ) by varying the volumetric flow rate (vvm) from the gas mixture 24% CO<sub>2</sub> in nitrogen and with a fixed amount of suspended carrier in the liquid (10%). (B) Gas-liquid CO<sub>2</sub> transfer rate ( $k_{La}$ ) by varying the percentage of resuspended Ni<sup>2+</sup> - ReliZyme in the medium at 1 vvm from the gas mixture 24% CO<sub>2</sub>.

Compared to oxygen (O<sub>2</sub>), for which  $k_{La}$  is typically measured, CO<sub>2</sub> generally has a lower  $k_{La}$  under standard conditions (25 °C and 1 atm). Under similar reaction conditions in this same reactor,  $k_{La(O_2)}$  can reach values up to an order of magnitude higher than  $k_{La(CO_2)}$  when air is directly bubbled into the system. Although CO<sub>2</sub> is more soluble than O<sub>2</sub> in water (0.033 vs. 0.001 mol L<sup>-1</sup>) under standard conditions (34), this results not only from physical dissolution but also from chemical interactions forming inorganic species that prolong CO<sub>2</sub> retention. (7) However, despite its higher solubility, CO<sub>2</sub> diffuses more



slowly than O<sub>2</sub> due to its larger molecular size, and chemical reactions that reduce the free View Article Online  
DOI: 10.1039/D6GC00387G

CO<sub>2</sub> available for transfer, leading to lower  $k_L a_{(\text{CO}_2)}$  values. (35)

In contrast, O<sub>2</sub> transfer is often limited by agitation, as increased stirring produces smaller bubbles and greater gas–liquid contact. In the case of CO<sub>2</sub>, its transfer is also limited by agitation, but even more so by the gas flow rate, as higher flow rates continuously renews the gas–liquid concentration gradient, thereby enhancing mass transfer and leading to higher  $k_L a_{(\text{CO}_2)}$  values. (36) However, at lower flow rates, mass transfer is slower, but rapid gas saturation is avoided, maintaining the concentration gradient longer and allowing more efficient gas utilization. In addition, gas bubbles also remain in contact with the liquid for a longer time, promoting more effective CO<sub>2</sub> utilization. (7,37) Although some studies suggest estimating  $k_L a_{(\text{CO}_2)}$  by multiplying  $k_L a_{(\text{O}_2)}$  by 0.91 attributed to physicochemical differences (38) , these gases have demonstrated different diffusion coefficients, so their transfer and absorption kinetics can differ even when bubbled together. (39) However, in this study,  $k_L a_{(\text{CO}_2)}$  was successfully determined in a stirred-tank reactor using a potentiometric sensor, enabling accurate and reliable measurements.

Importantly, this study of gas–liquid mass transfer provides a foundation for potentially incorporating key parameters into reactor-scale simulations for dynamic mass balance and reaction kinetics modeling. The measured  $k_L a$  values describe CO<sub>2</sub> transfer, allowing prediction of dissolved CO<sub>2</sub> profiles as a function of operating variables. These results pave the way for implementing gas-liquid mass transfer studies in other enzymatic CO<sub>2</sub> transformation including lactic acid production (22) and carboxylation, where reaction



kinetics depend strictly on CO<sub>2</sub> mass transfer and pH levels. Furthermore, this approach can be extended to other enzymatic processes involving gaseous substrates, such as oxidation reactions, which rely on maintaining optimal dissolved oxygen concentrations in the reaction medium.

### 3.2. Multi-enzymatic CO<sub>2</sub> reduction by evaluating different gas volumetric flow rates

The multi-enzymatic reduction of CO<sub>2</sub> into high-value compounds was assessed in a stirred-tank reactor by testing different volumetric flow rates (0.1, 0.5, and 1.0 vvm) of a gas mixture containing 24% CO<sub>2</sub>, which corresponds to the typical CO<sub>2</sub> content reported for the off-gases from blast furnaces in the iron and steel industry. (22) Although the effect of different immobilization carrier loadings on the determination of  $k_L a_{(CO_2)}$  was also evaluated, a 10% carrier-to-volume ratio was used in all these following reactions to ensure good distribution of the carrier in the liquid and to avoid the effect of excessive solids on CO<sub>2</sub> gas-liquid mass transfer. The concentrations of both enzymes (GC-GlyDH and FDH) in the biocatalyst were previously optimized by the authors, for both their free (14) and co-immobilized on Ni<sup>2+</sup>-ReliZyme forms. (15)

As a first point of comparison, it is important to understand the strong relationship between CO<sub>2</sub> flow rate and the pH resulting in the reaction medium. As previously explained, CO<sub>2</sub> reacts with water to form carbonic acid, which partially dissociates, releasing protons (H<sup>+</sup>) and thereby modulating the pH of the medium. (40) Therefore, higher CO<sub>2</sub> flow rates lead to increased CO<sub>2</sub> mass transfer rate and a more pronounced decrease in pH compared to lower flow rates. However, this close relationship is also influenced by key factors in the reaction medium, including buffer capacity, temperature



and partial pressure. (41) Figure S4 in SI shows a comparison of pH evolution over time for reactions at different vvm. At 1 vvm, the pH dropped sharply from 7.5 to 6.7 within one hour, then stabilized around pH 6.6. At 0.5 vvm, pH fell from 7.5 to 6.9 within one hour, then gradually to pH 6.7. At 0.1 vvm, the initial drop was minor, decreasing slowly from pH 7.3 to 7.0. Thus, the CO<sub>2</sub> dissolution rate governs pH changes over time, indicating that the three reactions occurred at different pH levels, which could potentially affect the reactions' microenvironment. Notably, accounting for the CO<sub>2</sub>-carbonate equilibrium is also essential for accurately predicting dissolved CO<sub>2</sub> concentrations as a function of medium pH, mass transfer rate and other operating parameters, particularly when extrapolating these effects to potential reactor-scale simulations. This approach has previously been validated for the development of mass transfer models, highlighting gas flow rate and CO<sub>2</sub> loading as the key factors influencing the mass transfer rate (42) as well as for models based on mechanistic enzymatic kinetic models, such as those describing carbonic anhydrase, under a range of operating conditions including temperature, CO<sub>2</sub> partial pressure and concentration. (43,44)

Regarding the multi-enzymatic CO<sub>2</sub> conversion reaction, Figure 4 presents the concentrations of formate, DHA, and glycerol carbonate, along with glycerol conversion, obtained after 80 h of reaction for the three evaluated volumetric flow rates. The time courses of the three reactions are illustrated in Figure S5 (SI). As observed, a linear correlation ( $R^2 > 0.99$ ) was found between the gas volumetric flow rate and each product concentrations, as well as glycerol conversion across all experiments, suggesting that CO<sub>2</sub> input and its concentration in the medium are key factors for the performance and efficiency of this multi-enzymatic system. Formate production was inversely proportional



to CO<sub>2</sub> input, with lower flow rates resulting in higher concentrations (Fig. 4A). At the lowest flow rate (0.1 vvm), and therefore at a pH closer to neutral (pH 7.0), the highest formate concentration was achieved,  $66.1 \pm 1.4$  mM (equivalent to 3 g L<sup>-1</sup>). This represents a 31.2% increase compared to the reaction conducted at 1 vvm ( $50.4 \pm 0.3$  mM). This result represents up to an 8.5-fold improvement over previous reports on enzymatic CO<sub>2</sub> reduction and cofactor regeneration platforms. (45–47) Similarly, this formate production is comparable to electrochemical and bioelectrocatalytic studies, where reported concentrations are similar or lower than those achieved in this work (48–50), highlighting the enhanced efficiency of the developed system. This milestone was accompanied by a 1.5-fold increase in the formate synthesis rate ( $0.66$  mM h<sup>-1</sup> at 1 vvm vs  $0.96$  mM h<sup>-1</sup> at 0.1 vvm), indicating enhanced catalytic performance under lower gas flow conditions. Accordingly, this constitutes the highest formate concentration reported to date via enzymatic synthesis.

For DHA, its concentration in the medium decreased as the gas volumetric flow rate was reduced (Fig. 4B), however, its low quantification in the liquid phase is attributed to its adsorption onto the biocatalyst with an adsorption capacity of 140.8 mg DHA g<sup>-1</sup>, as previously documented by the authors. (15) This effect arises from strong interactions between DHA and protein amino groups through the Maillard reaction. (51) Compared to the reaction at 1 vvm, which yielded a soluble DHA concentration of  $12.2 \pm 0.4$  mM, the reaction at 0.1 vvm showed only  $5.2 \pm 0.7$  mM, indicating that 92.1% of DHA produced was adsorbed onto the bifunctional biocatalyst (based on the equimolar formate co-production). This behavior may result from changes in the local microenvironment, such as reactor pressure, pH, or dissolved gas concentration, which can shift adsorption



equilibria. (52) Despite this significant adsorption, the authors also have reported the saturation of the biocatalyst over several reaction cycles, allowing greater accumulation of DHA in the liquid phase. Likewise, its desorption directly from the biocatalyst has also been demonstrated under mild conditions, achieving desorption yields of up to  $27.2 \pm 1.8\%$ . (15) However, further studies are needed to clarify the mechanisms driving this DHA adsorption and the contribution of each variable under these conditions.

Regarding glycerol carbonate, its concentration decreased as the gas flow rate was reduced (Fig. 4C). This may result from the multi-enzymatic reaction favoring formate synthesis at lower dissolved  $\text{CO}_2$  levels, leading glycerol to be preferentially consumed for DHA production rather than glycerol carbonate synthesis. However, no significant differences were observed in the GC production rate, suggesting that the intrinsic reaction kinetics for this compound were not substantially affected by the gas flow conditions. This indicates that the reaction was not limited by the gas–liquid mass transfer of  $\text{CO}_2$ . In the case of glycerol, its conversion increased with decreasing gas flow rate, reaching  $99.5 \pm 1.2\%$  at 0.1 vvm (Fig. 4D). Thus, optimizing reaction conditions can enhance substrate conversion and orientate the system toward improved formate and DHA enzymatic co-production.



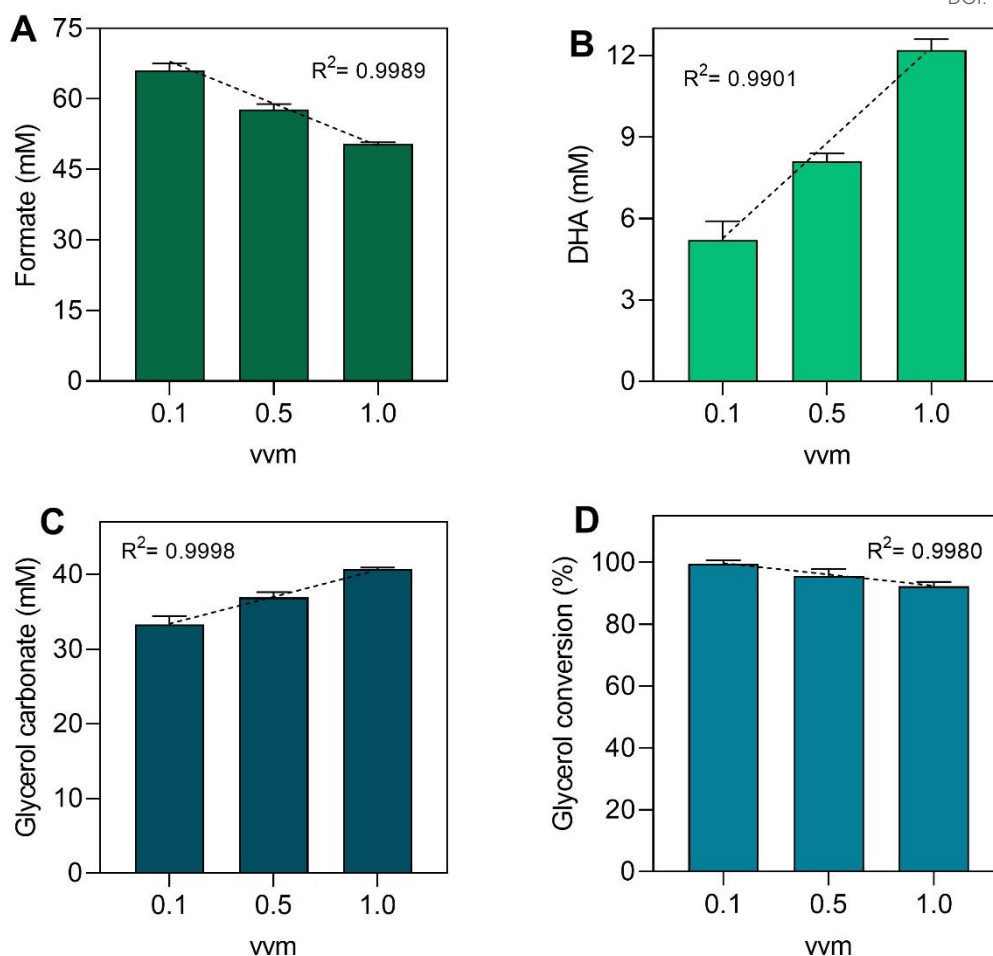


**Figure 4.** Multi-enzymatic reduction of CO<sub>2</sub> to high-value compounds using a bifunctional co-immobilized biocatalyst with *in situ* cofactor regeneration, evaluating three different gas volumetric flow rates from a 24% CO<sub>2</sub> gas mixture. (A) Formate [mM]. (B) DHA [mM]. (C) Glycerol carbonate [mM]. (D) Glycerol conversion [%]. *The DHA concentrations shown in this figure correspond only to the soluble fraction (not adsorbed onto the biocatalyst).*

Table S2 in SI presents some performance metrics obtained from the three reactions. At 0.1 vvm, a space-time yield (STY) for formate of  $37.2 \pm 2.2$  mg L<sup>-1</sup> h<sup>-1</sup> was determined, representing a 1.3-fold improvement compared to the reaction at 1 vvm. A similar improvement was observed in catalyst yield, which reached  $29.8 \pm 1.7$  mg formate per g



of biocatalyst. In the case of DHA and GC, these metrics decreased as the volumetric flow rate was reduced due to enhanced DHA adsorption on the biocatalyst and the shift of the reaction conditions to favor the co-production of formate and DHA while minimizing GC formation.

These remarkable findings can also be attributed to the sustained operational stability of the co-immobilized biocatalyst throughout the reaction, as observed in Figure 5. Notably, enzyme stability increased as the gas flow rate decreased, suggesting reduced inactivation at lower gas flow rate and dissolved CO<sub>2</sub> levels. At 0.1 vvm, GC-GlyDH and FDH retained 80.2 ± 2.1% and 96 ± 1.6% activity after 80 h, representing 1.9- and 1.8-fold improvements over the operational stability of the biocatalyst in the reaction at 1 vvm. This demonstrates the high biocatalyst's robustness and potential for reuse for consecutive reaction cycles under low dissolved CO<sub>2</sub> conditions. In addition, as mentioned earlier, changes in the reaction microenvironment can vary with gas supplementation, affecting parameters such as pH (Fig. S4 in SI). Since pH depends on dissolved CO<sub>2</sub> concentration, this can significantly influence enzyme stability. At slightly acidic pH (6.5–7.0), free GlyDH can lose up to 30% of its activity compared to pH 7.5, whereas free FDH loses only about 10%. (14) Additionally, even when immobilized, the enzymes may show slight pH-dependent inactivation, but much less than in their free form. (53) Consequently, lower dissolved CO<sub>2</sub> helped maintain near-neutral pH, enhancing enzyme stability and biocatalytic efficiency for formate production



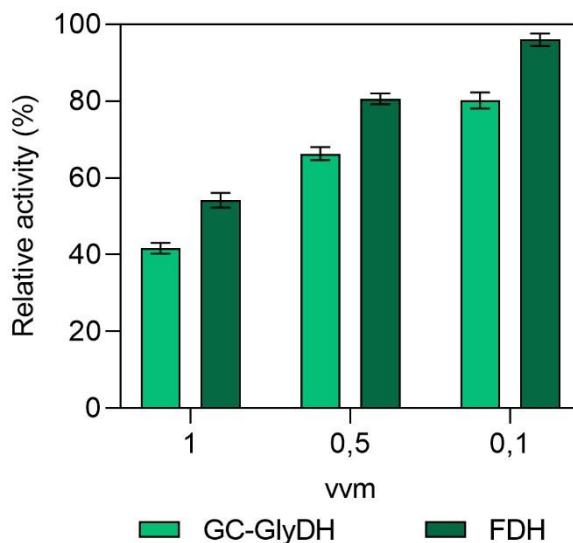


**Figure 5.** Operational stability of the bifunctional biocatalyst after 80 h of reaction corresponding to the multi-enzymatic reduction of CO<sub>2</sub> to high-value chemicals by evaluating three different gas volumetric flow rates using a 24% CO<sub>2</sub> gas mixture (1, 0.5 y 0.1 vvm). 100% relative activity was considered as the activity at the initial reaction time (time zero).

### 3.3. Carbon flow analysis in the CO<sub>2</sub> capture and utilization system

After evaluating the multi-enzymatic system at different gas flow rates, a mass balance was performed to quantify the CO<sub>2</sub> captured and converted, representing the fraction of emissions not released into the atmosphere. The setup included inlet, outlet, and dissolved CO<sub>2</sub> sensors, providing real-time measurements throughout the reaction. Figure S6 in SI shows the corresponding time-course data. At 1 vvm, dissolved CO<sub>2</sub> concentrations remained stable between 227–247 mg L<sup>-1</sup> (Fig. S6 A), indicating high gas turnover and steady substrate supply. At 0.5 vvm, the maximum CO<sub>2</sub> concentration was ~232 mg L<sup>-1</sup> but it gradually declined after 50 h, reaching 145 mg L<sup>-1</sup> by the end of the reaction. A similar behavior was observed at 0.1 vvm, where the maximum CO<sub>2</sub> concentration was



only  $\sim 214 \text{ mg L}^{-1}$ , followed by a steady decline at 48 h and stabilizing during the final two h at around  $\sim 36 \text{ mg L}^{-1}$ , reflecting a slower gas renewal rate. Despite this,  $\text{CO}_2$  remained sufficient to sustain the multi-enzymatic reaction (Fig. S5, SI). Regarding the decline in dissolved  $\text{CO}_2$  concentrations observed at 0.5 and 0.1 vvm, it likely reflects  $\text{CO}_2$  consumption exceeding gas replenishment, unlike at 1 vvm where renewal maintains stable levels (Fig. 6A). (54) Furthermore, as the reaction proceeds, rising fluid viscosity and foam formation can further limit gas–liquid mass transfer, especially at low gas flow rates. (55)

Regarding the gas inlet and outlet sensors, they operate via dual-wavelength infrared (IR) absorption to quantify  $\text{CO}_2$  in the gas phase. As shown in Figure S6 B, the inlet  $\text{CO}_2$  proportion remained steady at  $24.4 \pm 0.2\%$ , matching the gas mixture used in all experiments. However, although the inlet  $\text{CO}_2$  percentage was the same in all reactions, the actual amount of  $\text{CO}_2$  supplied varied with the gas flow rate. At 1 vvm, the outlet  $\text{CO}_2$  fraction remained stable at  $\sim 21.1 \pm 0.1\%$ , indicating  $\sim 3.4 \pm 0.5\%$  of  $\text{CO}_2$  was continuously dissolved into the medium. At 0.5 vvm, the outlet  $\text{CO}_2$  was  $\sim 19.8 \pm 0.9\%$  during the first 30 h, then gradually declined to  $\sim 16.4 \pm 0.5\%$ , reflecting more  $\text{CO}_2$  accumulation in the reaction system over time. At 0.1 vvm, the outlet  $\text{CO}_2$  initially increased to  $\sim 8.4 \pm 0.4\%$  and then steadily decreased after 30 h, reaching complete capture after 55 h, with no  $\text{CO}_2$  detected at the system outlet. This behavior reflects lower gas turnover, allowing more efficient  $\text{CO}_2$  capture and progressive consumption.



Based on the data collected from the gas sensors, the amount of non-emitted CO<sub>2</sub> (Captured fraction) throughout the reaction was determined. Table 1 summarizes the overall CO<sub>2</sub> mass balance, including the amounts of CO<sub>2</sub> supplied, captured, and converted (to formate and/or glycerol carbonate), as well as the yields at each stage. As observed, only  $13.8 \pm 1.3\%$  of the CO<sub>2</sub> supplied was captured within the system during the reaction conducted at 1 vvm, whereas at 0.5 vvm the CO<sub>2</sub> retention nearly doubled to  $24.4 \pm 0.9\%$ . This implies that some CO<sub>2</sub> remains in the system, either physically trapped, chemically absorbed (mainly as bicarbonate and other inorganic species), or unconverted due to reaction limitations. In the case of the reaction at 0.1 vvm, an exceptional capture efficiency of  $93.3 \pm 2.1\%$  was achieved, indicating that the decreased gas–liquid interfacial saturation at low volumetric flow rates resulted in a significant improvement in CO<sub>2</sub> retention within the system for its subsequent conversion. Under these conditions, conversion performance was also favored, where nearly the entire amount of CO<sub>2</sub> captured was converted into the target products, reaching production yields of  $0.84 \pm 0.07$  g of formate and  $1.09 \pm 0.06$  g of GC (as the total molecule) per g of CO<sub>2</sub> captured at 0.1 vvm. Thus, although more CO<sub>2</sub> is captured at 1 vvm, the multi-enzymatic system was favored by the improved biocatalyst performance at near-neutral pH at 0.1 vvm, thereby maximizing the utilization of the captured CO<sub>2</sub>. Despite this, the amount of CO<sub>2</sub> converted into products was similar across all reactions, suggesting that conversion is the limiting step of this system.

View Article Online  
DOI: 10.1039/D6GC00387G





**Table 1.** Material balance and performance metrics for CO<sub>2</sub> capture and conversion in the multi-enzymatic reduction process to high value-added compounds. Experiments were conducted at three different volumetric gas flow rates using a 24% CO<sub>2</sub> gas mixture in a stirred-tank reactor with a 200 mL reaction volume. *GC: Glycerol carbonate.*

Volumetric gas flow rate (vvm)	Supplied CO <sub>2</sub> (g)	Captured CO <sub>2</sub> (g)	Capture efficiency (%)	Converted CO <sub>2</sub> (g)*	Product yield (g product g CO <sub>2</sub> <sup>-1</sup> ) **	
					Formate	GC
1	7.74 ± 0.23	1.07 ± 0.18	13.8 ± 1.3	0.81 ± 0.13	0.43 ± 0.09	0.90 ± 0.08
0.5	3.87 ± 0.14	0.95 ± 0.08	24.4 ± 0.9	0.84 ± 0.14	0.56 ± 0.04	0.92 ± 0.09
0.1	0.77 ± 0.11	0.72 ± 0.12	93.3 ± 2.1	0.89 ± 0.08	0.84 ± 0.07	1.09 ± 0.06

\* Corresponding to the fraction of CO<sub>2</sub> atoms incorporated into formate and glycerol carbonate.

\*\* Based on the total mass of each product.

Based on CO<sub>2</sub> conversion to the target products, Table 2 summarizes key performance metrics for this stage. As observed, enzymatic selectivity for formate increases as the gas flow rate decreases ( $82.5 \pm 2.4\%$  at 0.1 vvm), showing more efficient enzymatic CO<sub>2</sub> utilization at neutral pH. In the case of GC, its non-enzymatic production was less selective, especially at 0.1 vvm, where formate yield was roughly twice that of GC. At 0.1 vvm, all captured CO<sub>2</sub> was efficiently converted into formate and GC, obtaining an overall selectivity of  $123.1 \pm 2.2\%$ . This apparent overestimation likely arises from the error linked to the determination of captured CO<sub>2</sub> ( $0.72 \pm 0.12$  g) which represents almost a 17% of error, combined with the accuracy of the flow meter and gas sensors, particularly when operating at low flow rates. Nonetheless, despite this, the global selectivity in each reaction was considerably high, as the system allowed for the maximization of CO<sub>2</sub> utilization to produce both products.

In terms of carbon efficiency, only  $10.5 \pm 0.7\%$  of the supplemented CO<sub>2</sub> at 1 vvm was converted into the target products (formate and GC), while at 0.5 vvm roughly doubled to  $21.8 \pm 1.1\%$ . Remarkably, at 0.1 vvm, all supplied CO<sub>2</sub> was converted into the target products ( $114.7 \pm 1.6\%$ ), indicating maximal utilization of the total supplemented CO<sub>2</sub>. The slight overestimation likely reflects the previously mentioned sources of errors. Under these conditions, glycerol was also almost completely consumed, with a conversion yield of  $99.5 \pm 1.2\%$  (Fig. 4D). Therefore, the inclusion of an additional CO<sub>2</sub> and glycerol valorization route in this multi-enzymatic system, the synthesis of glycerol carbonate, enhanced the overall carbon efficiency and expanded the products portfolio of this process, thus also contributing to overall process sustainability by generating an



additional high-value product from the same feedstocks. Likewise, the potential for developing reactor-scale predictive models based on these operation conditions requires explicit consideration of pH-dependent CO<sub>2</sub> speciation when coupling gas–liquid mass transfer with reaction kinetics. **As result**, this would enable a more realistic description of CO<sub>2</sub> behavior and availability within the system, ensuring adequate gas supply for the reaction while maximizing conversion efficiency in greener biocatalytic processes.

**Table 2.** Performance metrics of CO<sub>2</sub> conversion into high-value products, formate and glycerol carbonate (GC), evaluated at different volumetric gas flow rates (1, 0.5 and 0.1 vvm) of a 24% CO<sub>2</sub> gas mixture in a multi-enzymatic system.

Volumetric gas flow rate (vvm)	Selectivity (%)		Global process selectivity (%)	Carbon efficiency (%)
	Formate	GC		
1	42.4 ± 1.3	33.5 ± 0.8	75.9 ± 1.1	10.5 ± 0.7
0.5	55.1 ± 1.7	34.4 ± 1.5	89.5 ± 1.6	21.8 ± 1.1
0.1	82.5 ± 2.4	40.6 ± 1.8	123.1 ± 2.2	114.7 ± 1.6

Several studies have shown successful CO<sub>2</sub> capture and conversion into value-added products. Zhou *et al.* demonstrated the production of methane from CO<sub>2</sub> with complete capture and conversion efficiency (100%) using a fixed-bed reactor packed with adsorbents specifically designed for CO<sub>2</sub>. (56) The same reactor, operated in different configurations, has also been widely used to produce various chemicals and fuels from industrial gas streams, achieving capture efficiencies over 85%. (57) On the other hand, CO<sub>2</sub> capture using the regenerative ammonia method has reported efficiencies exceeding 90% for the direct production of fertilizers from CO<sub>2</sub> (58) , and capturing CO<sub>2</sub> as carbamic



acid from amino acid salts has also been shown to be a feasible strategy for CO<sub>2</sub> utilization to produce compounds such as oxazolidinones. (59) Additionally, among the simplest capture methods, solvent-based approaches have achieved efficiencies above 90% using solvents like monoethanolamine (MEA), 2-amino-2-methyl-1-propanol (AMP), and piperazine (PZ). (60) However, CO<sub>2</sub> conversion in these systems is often limited by solvent degradation, impurities, and the reduced reactivity of CO<sub>2</sub> caused by the formation of stable amine complexes. (61) Finally, although electrochemical systems often achieve high CO<sub>2</sub> conversion rates exceeding 95%, this performance frequently comes at the expense of low selectivity, increased energy requirements and CO<sub>2</sub> supplementation with low capture efficiencies. (62,63)

In the case of enzymatic processes, CO<sub>2</sub> conversion rates are often not reported, mainly due to measurement challenges, the involvement of other inorganic substrates, and the common practice of estimating yields from NADH consumption, as typically done in FDH-catalyzed reactions. However, a study reported a CO<sub>2</sub> conversion to formate efficiency of 80.5% using FDH immobilized on metal-organic frameworks (MOFs), markedly improving the enzyme's catalytic performance. (64) Additionally, complete (100%) conversion of CO<sub>2</sub> from industrial off-gases to formate by FDH was also reported, highlighting the potential of these systems for efficient valorization of gas emissions, even at low CO<sub>2</sub> concentrations. (65) In multi-enzymatic systems, CO<sub>2</sub> reduction has been successfully applied to produce compounds such as pyruvate, achieving conversion of 81%. (66) In contrast, methanol production generally shows much lower CO<sub>2</sub> conversion efficiencies, mainly due to the complexity of multiple sequential enzymatic reduction



steps, with reported values ranging from 3% to 25% (67,68), highlighting the challenges in optimizing these multi-step biocatalytic processes. Finally, carbonic anhydrase has been shown to selectively accelerate CO<sub>2</sub> capture up to 20-fold, while also promoting its conversion into compounds such as carbon monoxide and carbonates, reaching yields of approximately 80% or higher. (6,69) In addition, its synergy with FDH enzymes has been effectively demonstrated to enhance the CO<sub>2</sub> conversion to formate. (46,47) Overall, enzymes represent a feasible biocatalytic tool for the development of sustainable processes aimed at CO<sub>2</sub> capture and conversion into value-added industrial products.

### 3.4. Environmental implications of the multi-enzymatic CO<sub>2</sub> reduction system

Once the CO<sub>2</sub> conversion performance was evaluated, the environmental impact of these processes was also analyzed. As extensively reported, the enzymatic reduction of CO<sub>2</sub> represents a green and sustainable catalytic route for mitigating greenhouse gas emissions. (70,71) Since enzymes originate from renewable biological systems, they are inherently biocompatible and environmentally benign, offering a safer alternative to heavy-metal and synthetic complex catalysts. Consequently, enzymatic catalysis stands out as a key strategy for advancing carbon-neutral bioprocessing and sustainable industrial chemistry. (72) However, to the best of our knowledge, only few reports have evaluated the environmental impact of these enzymatic processes. Therefore, to evaluate the greenness of this multi-enzymatic reaction, the Global Warming Potential (GWP) was estimated both in terms of the materials used for the production and the energy invested in each reaction carried out at different volumetric gas flow rates (Fig. 6).



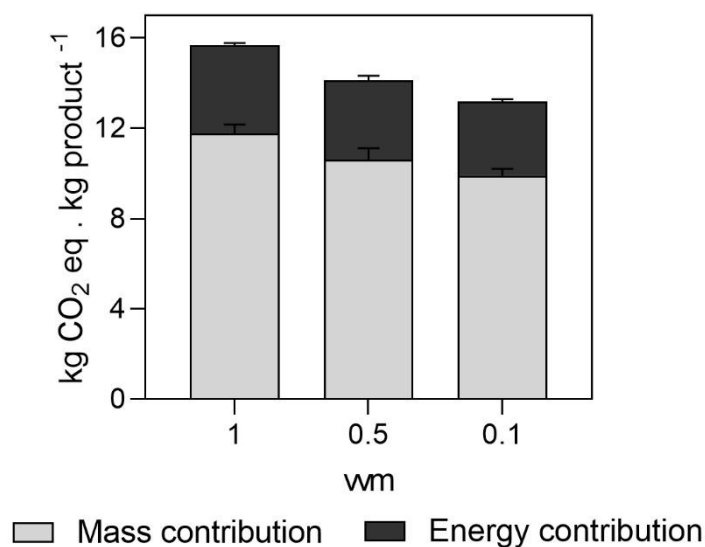


**Figure 6.** Total Global Warming Potential (GWP) assessment of the multi-enzymatic reduction of CO<sub>2</sub> to high value-added compounds (accounting for formate, DHA and GC), varying the inlet volumetric gas flow rate from a 24% CO<sub>2</sub> gas mixture.

A clear correlation was observed between the applied volumetric gas flow rate and the global warming contribution. At the lowest flow rate (0.1 vvm), CO<sub>2</sub> conversion was highest, indicating that maximizing multi-enzymatic carbon utilization can significantly reduce the environmental footprint of the process due to more efficient use of resources.

In this reaction, a total GWP of  $13.2 \pm 0.2$  kg CO<sub>2</sub> eq per kg of product was obtained.

Compared to electrochemical CO<sub>2</sub> reduction platforms, some processes can exhibit an environmental impact at least 1.5 times greater than that observed in this study. (73–75)

This is mainly due to their high energy consumption, the materials required for electrodes and electrolytes, and their rapid degradability, which generates additional waste.

However, in some cases, the optimization of these processes at industrial scales can substantially improve their environmental footprint (up to four times lower than in this



study). (76,77) . Regarding these enzymatic platforms, information on their environmental performance remains limited; nevertheless, the present study provides a foundational dataset that can be used to further develop a comprehensive Life Cycle Assessment (LCA).

On the other hand, the energy demand and conversion losses associated with fossil-based processes can lead to a higher global warming impact compared to CO<sub>2</sub>-based processes, where different amounts of products can be obtained directly from CO<sub>2</sub> (78) , as demonstrated in this study. Consequently, renewable-based systems are considered the most promising candidates for achieving negative greenhouse gases (GHG) emissions. (79) As a result, a CO<sub>2</sub> capture and conversion system was successfully developed by investigating the gas-liquid mass transfer of CO<sub>2</sub> and implementing a sensor-based approach to accurately quantify the amount of CO<sub>2</sub> that was prevented from being emitted into the atmosphere and effectively converted into valuable industrial molecules. These findings pave the way for the development of large-scale sustainable multi-enzymatic systems and the establishment of benchmarks such as industrial feedstock valorization, CO<sub>2</sub> capture and conversion efficiency, robust biocatalyst stability, and reduced environmental impact, which could serve as key criteria for identifying promising strategies that make a substantial contribution to GHG mitigation and advance green chemistry and CCU technologies

#### 4. CONCLUSIONS



The gas–liquid transfer of CO<sub>2</sub> in the multi-enzymatic system was successfully evaluated in a stirred-tank reactor using reactor engineering to gain insights into CO<sub>2</sub> mass transfer during the stages of capture and conversion and enabling a first assessment of the sustainability of this type of bioprocess. The volumetric mass transfer coefficient ( $k_L a$ ) was determined with a digital in-line CO<sub>2</sub> sensor based on pH under different gas flow rates from a 24% CO<sub>2</sub> gas mixture, showing that higher flow rates increased CO<sub>2</sub> transfer when the system operated with 10% immobilization carrier resuspended. At the lowest volumetric gas flow rate (0.1 vvm), the multi-enzymatic reaction achieved the highest formate concentration reported to date by an enzymatic route,  $66.1 \pm 1.4$  mM. This was attributed to pH shifts from CO<sub>2</sub> dissolution, which improved biocatalyst stability at near-neutral pH and revealed a strong correlation between pH and CO<sub>2</sub> transfer rate, significantly influencing the biocatalytic transformation. Finally, the mass balance showed that a portion of the supplied CO<sub>2</sub> was effectively retained, avoiding its release to the atmosphere, with the highest capture efficiency at 0.1 vvm ( $93.3 \pm 2.1\%$ ). Moreover, although a higher amount of CO<sub>2</sub> was captured at 1 vvm, all CO<sub>2</sub> captured at 0.1 vvm was selectively converted into value-added products (formate and glycerol carbonate) demonstrating the high efficiency of the multi-enzymatic system for CO<sub>2</sub> valorization, facilitated by significantly improved reaction conditions at 0.1 vvm. Thus, evaluating gas flow rate provided key insights into CO<sub>2</sub> gas–liquid transfer, directly enhancing enzyme-driven carbon utilization at low CO<sub>2</sub> concentrations. These insights provide a foundation for further reactor-scale simulations predicting CO<sub>2</sub> behavior based on pH-dependent speciation, mass transfer rates, and other key operating variables under these conditions. Furthermore, the environmental impact assessment highlights

View Article Online  
DOI: 10.1039/D6GC00387G



enzymatic CO<sub>2</sub> reduction systems as promising and viable strategies for industrial implementation within conventional manufacturing processes, achieving a substantial reduction in the environmental impact of this system, afforded by maximal CO<sub>2</sub> utilization for the production of the target products.

View Article Online  
DOI: 10.1039/D6GC00387G

### Author contributions

S.R.R. contributed to data curation, formal analysis, investigation and writing the original draft. The project, conceptualized by M.G. and O.R., involved activities such as funding acquisition, project administration, and methodological development. Additionally, M.G. and O.R., were actively engaged in validating, supervising, visualizing, reviewing, and editing this manuscript.

### Conflicts of interest

There are no conflicts to declare

### Data availability

All datasets generated or analyzed during this study are available at <https://doi.org/10.34810/data2645>. Supplementary information: Experimental procedures for the co-immobilization of FDH and GlyDH enzymes, activity assays, protein content measurement, and HPLC analysis. Equations for the response time of the dissolved CO<sub>2</sub> sensor, its operating diagram, and the CO<sub>2</sub> mass balance equations. Scheme of the reaction mechanism for GC formation. Results of the determination of the response time of the dissolved CO<sub>2</sub> sensor, determination of the volumetric mass transfer



coefficient ( $k_L a$ ) of CO<sub>2</sub> under different conditions, performances metrics of yields and productivity, pH monitoring, time-course of substrates and products, and monitoring of dissolved CO<sub>2</sub> concentrations and inlet/outlet CO<sub>2</sub> fractions during multi-enzymatic CO<sub>2</sub> reduction reactions.

### Acknowledgments.

S.R.R. acknowledges the Generalitat of Catalunya (AGAUR) for his pre-doctoral scholarship (Joan Oro – 2022FI\_B 00955). All the authors acknowledge Generalitat de Catalunya, and the 2021 SGR 00143 and project MEPLAB-CO<sub>2</sub> (TED2021-129732A-I00) funded by MCIN/AEI/10.13039/501100011033 and by the European Union "NextGenerationEU"/PRTR.

### REFERENCES

1. Che Ramli ZA, Pasupuleti J, Samidin S, Wan Isahak WNR, Sofiah AGN, Koh SP. An overview of the conversion technologies of CO<sub>2</sub> into active CO molecule: Reactor engineering, reaction pathways, product purification and upgrading. *Int J Hydrogen Energy*. 2025 Aug;157:150374. doi:10.1016/j.ijhydene.2025.150374
2. Buckingham J, Reina TR, Duyar MS. Recent advances in carbon dioxide capture for process intensification. *Carbon Capture Sci Technol*. 2022 Mar;2:100031. doi:10.1016/j.ccst.2022.100031
3. Lin J, Zhang Y, Xu P, Chen L. CO<sub>2</sub> electrolysis: Advances and challenges in electrocatalyst engineering and reactor design. *Materials Reports: Energy*. 2023 May;3(2):100194. doi:10.1016/j.matre.2023.100194
4. Ola O, Maroto-Valer MM. Review of material design and reactor engineering on TiO<sub>2</sub> photocatalysis for CO<sub>2</sub> reduction. *J Photochem Photobiol C: Photochem Rev.s*. 2015 Sep;24:16–42. doi:10.1016/j.jphotochemrev.2015.06.001
5. Ding X, Liu W, Zhao J, Wang L, Zou Z. Photothermal CO<sub>2</sub> Catalysis toward the Synthesis of Solar Fuel: From Material and Reactor Engineering to



Techno-Economic Analysis. *Advanced Materials*. 2025 Jan 7;37(2). View Article Online  
DOI: 10.1039/D6GC00387G  
doi:10.1002/adma.202312093

6. Talekar S, Jo BH, Dordick JS, Kim J. Carbonic anhydrase for CO<sub>2</sub> capture, conversion and utilization. *Curr Opin Biotechnol*. 2022 Apr;74:230–40. doi:10.1016/j.copbio.2021.12.003
7. Ndiaye M, Gadoin E, Gentric C. CO<sub>2</sub> gas–liquid mass transfer and kLa estimation: Numerical investigation in the context of airlift photobioreactor scale-up. *Chem Eng Res Des*. 2018 May;133:90–102. doi:10.1016/j.cherd.2018.03.001
8. Garcia-Ochoa F, Gomez E. Bioreactor scale-up and oxygen transfer rate in microbial processes: An overview. *Biotechnol Adv*. 2009 Mar;27(2):153–76. doi:10.1016/j.biotechadv.2008.10.006
9. Zhao L, Hu HY, Wu AG, Terent'ev AO, He LN, Li HR. CO<sub>2</sub> capture and in-situ conversion to organic molecules. *J CO<sub>2</sub> Util*. 2024 Apr;82:102753. doi:10.1016/j.jcou.2024.102753
10. Puskeiler R, Edler M, Didzus K, Müller R, Gabelsberger J. Mass Transfer Considerations for Scale-Up and Scale-Down of Animal Cell Bioprocesses. In: *Proceedings of the 21st Annual Meeting of the European Society for Animal Cell Technology (ESACT), Dublin, Ireland, June 7-10, 2009*. Dordrecht: Springer Netherlands; 2012. p. 451–4. doi:10.1007/978-94-007-0884-6\_77
11. Valdés FJ, Hernández MR, Catalá L, Marcilla A. Estimation of CO<sub>2</sub> stripping/ CO<sub>2</sub> microalgae consumption ratios in a bubble column photobioreactor using the analysis of the pH profiles. Application to *Nannochloropsis oculata* microalgae culture. *Bioresour Technol*. 2012 Sep;119:1–6. doi:10.1016/j.biortech.2012.05.120
12. Graham Walker J. Development of Mass Transfer Coefficient Correlations Between Carbon Dioxide and Oxygen for Air-lift Devices [All Theses. 4155.] [Internet]. Master of Science Biosystems Engineering. Clemson University; 2023 [cited 2025 Jul 31]. Available from: [https://open.clemson.edu/all\\_theses/4155](https://open.clemson.edu/all_theses/4155)
13. Adnan AI, Ong MY, Nomanbhay S, Show PL. Determination of Dissolved CO<sub>2</sub> Concentration in Culture Media: Evaluation of pH Value and Mathematical Data. Processes. 2020 Oct 29;8(11):1373. doi:10.3390/pr8111373
14. Rodriguez SR, Álvaro G, Guillén M, Romero O. Multienzymatic Platform for Coupling a CCU Strategy to Waste Valorization: CO<sub>2</sub> from the Iron and Steel Industry and Crude Glycerol from Biodiesel Production. *ACS Sustain Chem Eng*. 2025 Jan 17;13(4):1440–9. doi:10.1021/acssuschemeng.4c04908
15. Rodriguez SR, Romero O, Guillén M. Enzyme-Powered CO<sub>2</sub> Utilization: A Bifunctional Immobilized Biocatalyst for Intensified CCU of Industrial Feedstocks



- to High-Value Chemicals. *ACS Sustain Chem Eng.* 2025 Dec 23. doi:10.1021/acssuschemeng.5c07343
16. Amao Y. Formate dehydrogenase for CO<sub>2</sub> utilization and its application. *J CO<sub>2</sub> Util.* 2018 Jul 1;26:623–41. doi:10.1016/j.jcou.2018.06.022
17. Thijs B, Rongé J, Martens JA. Matching emerging formic acid synthesis processes with application requirements. *Green Chem.* 2022;24(6):2287–95. doi:10.1039/D1GC04791D
18. Tomatis M, Kumar Jeswani H, Azapagic A. Environmental impacts of valorisation of crude glycerol from biodiesel production – A life cycle perspective. *Waste Manag.* 2024 Apr;179:55–65. doi:10.1016/j.wasman.2024.03.005
19. Bricotte L, Chougrani K, Alard V, Ladmiral V, Caillol S. Dihydroxyacetone: A User Guide for a Challenging Bio-Based Synthon. *Molecules.* 2023 Mar 17;28(6):2724. doi:10.3390/molecules28062724
20. Lukato S, Kasozi GN, Naziriwo B, Tebandeke E. Glycerol carbonylation with CO<sub>2</sub> to form glycerol carbonate: A review of recent developments and challenges. *Curr Res Green Sustain Chem.* 2021 Jan 1;4. doi:10.1016/j.crgsc.2021.100199
21. Ke YH, Xu H, Wang X, Liu H, Yuan H. Production of glycerol carbonate by coupling glycerol and CO<sub>2</sub> over various metal oxide catalyst. *J CO<sub>2</sub> Util.* 2024 May;83:102813. doi:10.1016/j.jcou.2024.102813
22. Carceller A, Guillén M, Álvaro G. Lactic Acid from CO<sub>2</sub>: A Carbon Capture and Utilization Strategy Based on a Biocatalytic Approach. *Environ Sci Technol.* 2023 Dec 26;57(51):21727–35. doi:10.1021/acs.est.3c05455 PubMed PMID: 38078668.
23. Gao J, Yang JW, Ma T, Wang J, Xia D, Du B, et al. Mechanism study on direct synthesis of glycerol carbonate from CO<sub>2</sub> and glycerol over shaped CeO<sub>2</sub> model catalysts. *Chin Chem Lett.* 2023 Dec;34(12):108395. doi:10.1016/j.ccllet.2023.108395
24. Belsa B, Xia L, García de Arquer FP. CO<sub>2</sub> Electrolysis Technologies: Bridging the Gap toward Scale-up and Commercialization. *ACS Energy Lett.* 2024 Sep 13;9(9):4293–305. doi:10.1021/acsenerylett.4c00955
25. Constable DJC, Curzons AD, Cunningham VL. Metrics to ‘green’ chemistry— which are the best? *Green Chem.* 2002;4(6):521–7. doi:10.1039/B206169B
26. Domínguez de María P. General equations to estimate the CO<sub>2</sub> production of (bio)catalytic reactions in early development stages. *RSC Sustainability.* 2024;2(12):3817–25. doi:10.1039/D4SU00535J
27. Kordač M, Linek V. Dynamic measurement of carbon dioxide volumetric mass transfer coefficient in a well-mixed reactor using a pH probe: Analysis of the salt



and supersaturation effects. *Ind Eng Chem Res.* 2008 Feb 20;47(4):1310-7. doi:10.1021/ie0711776

28. Akkarawatkhoosith N, Nopcharoenkul W, Kaewchada A, Jaree A. Mass Transfer Correlation and Optimization of Carbon Dioxide Capture in a Microchannel Contactor: A Case of CO<sub>2</sub>-Rich Gas. *Energies (Basel).* 2020 Oct 19;13(20):5465. doi:10.3390/en13205465
29. Mojica Prieto FJ, Millero FJ. The values of pK<sub>1</sub> + pK<sub>2</sub> for the dissociation of carbonic acid in seawater. *Geochim Cosmochim Acta.* 2002 Jul;66(14):2529–40. doi:10.1016/S0016-7037(02)00855-4
30. Tsukahara K, Okamura K, Noguchi T, Hatta M. Development of an acid extraction-NDIR method for the determination of total dissolved inorganic carbon using small sample volumes. *Galaxea J Coral Reef Stud.* 2025;27(1):G270-3. doi:10.3755/galaxea.G270-3
31. Moutafchieva D, Popova D, Dimitrova M, Tchaoushev S. Experimental determination of the volumetric mass transfer coefficient. *J Chem Technol Metall.* 2013;48(4):351–6.
32. Faasen DP, Sepahi F, Krug D, Verzicco R, Peñas P, Lohse D, et al. Diffusive and convective dissolution of carbon dioxide in a vertical cylindrical cell. *Phys Rev Fluids.* 2023 Sep;8(9):093501. doi:https://doi.org/10.1103/PhysRevFluids.8.093501
33. Gonçalves AL, Almeida F, Rocha FA, Ferreira A. Improving CO<sub>2</sub> mass transfer in microalgal cultures using an oscillatory flow reactor with smooth periodic constrictions. *J Environ Chem Eng.* 2021 Dec 1;9(6). doi:10.1016/j.jece.2021.106505
34. Khajooie S, Gaus G, Seemann T, Ahrens B, Hua T, Littke R. Exploring Effective Diffusion Coefficients in Water-Saturated Reservoir Rocks via the Pressure Decay Technique: Implications for Underground Hydrogen Storage. *Transp Porous Media.* 2025 Feb 8;152(2):12. doi:10.1007/s11242-024-02148-y
35. Aitchison TF, Timmons MB, Bisogni JJ, Piedrahita RH, Vinci BJ. Using Oxygen Gas Transfer Coefficients to Predict Carbon Dioxide Removal. *Int J Recirc Aquac.* 2007 Jun 1;8(1). doi:10.21061/ijra.v8i1.1416
36. Nickel N, Fitschen J, Haase I, Kuschel M, Schulz TW, Wucherpfennig T, et al. Novel sparging strategies to enhance dissolved carbon dioxide stripping in industrial scale stirred tank reactors. *Front Chem Eng.* 2024 Nov 15;6. doi:10.3389/fceng.2024.1470991
37. Nedeltchev S. Updated Review on the Available Methods for Measurement and Prediction of the Mass Transfer Coefficients in Bubble Columns. *Fluids.* 2025 Jan 27;10(2):29. doi:10.3390/fluids10020029



38. Uyar B, Ali MD, Uyar GEO. Design parameters comparison of bubble column airlift and stirred tank photobioreactors for microalgae production. *Bioprocess Biosyst Eng.* 2024 Feb 16;47(2):195–209. doi:10.1007/s00449-023-02952-8
39. Polat HM, Coelho FM, Vlugt TJH, Mercier Franco LF, Tsimpanogiannis IN, Moulton OA. Diffusivity of CO<sub>2</sub> in H<sub>2</sub>O: A Review of Experimental Studies and Molecular Simulations in the Bulk and in Confinement. *J Chem Eng Data.* 2024 Oct 10;69(10):3296–329. doi:10.1021/acs.jced.3c00778
40. Antonopoulou I, de Oliveira Maciel A, Di Giacomo M, Russo ME, Rova U, Christakopoulos P, et al. Accelerated carbonate weathering by immobilized recombinant carbonic anhydrase. *Journal of CO<sub>2</sub> Utilization.* 2025 Apr;94:103050. doi:10.1016/j.jcou.2025.103050
41. Mohammadian E, Hadavimoghaddam F, Kheirollahi M, Jafari M, Chenlu X, Liu B. Probing Solubility and pH of CO<sub>2</sub> in aqueous solutions: Implications for CO<sub>2</sub> injection into oceans. *J CO<sub>2</sub> Util.* 2023 May;71:102463. doi:10.1016/j.jcou.2023.102463
42. Wang R, Ni L, Zhang N, Li Q, An S, Wang L. Predictive model for CO<sub>2</sub> absorption and mass transfer process based on machine learning methods. *Sep Purif Technol.* 2025 Aug;366:132584. doi:10.1016/j.seppur.2025.132584
43. Gladis A, Gundersen MT, Neerup R, Fosbøl PL, Woodley JM, von Solms N. CO<sub>2</sub> mass transfer model for carbonic anhydrase-enhanced aqueous MDEA solutions. *Chem Eng J.* 2018 Mar;335:197–208. doi:10.1016/j.cej.2017.10.111
44. Shen Y, Shao P, Zhao J, Lu Y, Zhang S. Mass Transfer-Reaction Modeling of CO<sub>2</sub> Capture Mediated by Immobilized Carbonic Anhydrase Enzyme on Multiscale Supporting Structures. *Environ Sci Technol.* 2025 Feb 4;59(4):1995–2005. doi:10.1021/acs.est.4c09673
45. Pietricola G, Tommasi T, Dosa M, Camelin E, Berruto E, Ottone C, et al. Synthesis and characterization of ordered mesoporous silicas for the immobilization of formate dehydrogenase (FDH). *Int J Biol Macromol.* 2021 Apr;177:261–70. doi:10.1016/j.ijbiomac.2021.02.114
46. Sato R, Amao Y. Carbonic anhydrase/formate dehydrogenase bienzymatic system for CO<sub>2</sub> capture, utilization and storage. *React Chem Eng.* 2022;7(1):181–91. doi:10.1039/D1RE00405K
47. Li Y, Wen L, Tan T, Lv Y. Sequential Co-immobilization of Enzymes in Metal-Organic Frameworks for Efficient Biocatalytic Conversion of Adsorbed CO<sub>2</sub> to Formate. *Front Bioeng Biotechnol.* 2019 Dec 6;7. doi:10.3389/fbioe.2019.00394
48. Yan L, Liu G, Liu J, Bai J, Li Y, Chen H, et al. Hierarchically porous metal organic framework immobilized formate dehydrogenase for enzyme electrocatalytic CO<sub>2</sub> reduction. *Chem Eng J.* 2022 Dec 15;450:138164. doi:10.1016/j.cej.2022.138164



49. Kim SH, Chung GY, Kim SH, Vinothkumar G, Yoon SH, Jung KD. Electrochemical NADH regeneration and electroenzymatic CO<sub>2</sub> reduction on Cu nanorods/glassy carbon electrode prepared by cyclic deposition. *Electrochim Acta*. 2016 Aug 20;210:837–45. doi:10.1016/j.electacta.2016.06.007
50. Maureira D, Rodriguez SR, Romero O, Guillén M, Álvaro G, Wilson L, et al. Immobilization of FDH on carbon felt by affinity binding strategy for CO<sub>2</sub> conversion. *Results Eng*. 2025 Mar 1;25:104442. doi:10.1016/j.rineng.2025.104442
51. Sun Y, Al-Zahrani FAM, Lin L. Colour formation of dihydroxyacetone with cysteine and its derivatives via Maillard reaction. *Dyes and Pigments*. 2022 Dec 1;208. doi:10.1016/j.dyepig.2022.110854
52. Wasilewska M, Derylo-Marczewska A, Marczewski AW. Comprehensive Studies of Adsorption Equilibrium and Kinetics for Selected Aromatic Organic Compounds on Activated Carbon. *Molecules*. 2024 Apr 28;29(9):2038. doi:10.3390/molecules29092038
53. Chalella Mazzocato M, Jacquier JC. Recent Advances and Perspectives on Food-Grade Immobilisation Systems for Enzymes. *Foods*. 2024 Jul 3;13(13):2127. doi:10.3390/foods13132127
54. Gladis AB. PhD thesis: Upscaling of enzyme enhanced CO<sub>2</sub> capture [Internet]. [Kongens Lyngby]: Center for Energy Resources Engineering. Technical University of Denmark; 2017 [cited 2025 Aug 10]. Available from: <https://orbit.dtu.dk/en/publications/upscaling-of-enzyme-enhanced-co2-capture>
55. Sheng L, Chang Y, Deng J, Luo G. Hydrodynamics and mass transfer performance of gas–liquid microflow in viscous liquids. *Chem Eng J*. 2023 Feb;454:140407. doi:10.1016/j.cej.2022.140407
56. Zhou Z, Sun N, Wang B, Han Z, Cao S, Hu D, et al. 2D-Layered Ni–MgO–Al<sub>2</sub>O<sub>3</sub> Nanosheets for Integrated Capture and Methanation of CO<sub>2</sub>. *ChemSusChem*. 2020 Jan 19;13(2):360–8. doi:10.1002/cssc.201902828
57. Shao B, Zhang Y, Sun Z, Li J, Gao Z, Xie Z, et al. CO<sub>2</sub> capture and in-situ conversion: recent progresses and perspectives. *Green Chem Eng*. 2022 Sep;3(3):189–98. doi:10.1016/j.gce.2021.11.009
58. Fu L, Ren Z, Si W, Ma Q, Huang W, Liao K, et al. Research progress on CO<sub>2</sub> capture and utilization technology. *J CO<sub>2</sub> Util*. 2022 Dec;66:102260. doi:10.1016/j.jcou.2022.102260
59. Liu A, Ma R, Song C, Yang Z, Yu A, Cai Y, et al. Equimolar CO<sub>2</sub> Capture by N-Substituted Amino Acid Salts and Subsequent Conversion. *Angew Chem Int Ed*. 2012 Nov 5;51(45):11306–10. doi:10.1002/anie.201205362



60. Chen YM, Hsu HJ, Lin YJ. Improving CO<sub>2</sub> Capture Efficiency with High-Capacity Solvents: Addressing Temperature-Induced Mass Transfer Limitations. *Ind Eng Chem Res.* 2025 Jan 29;64(4):2283–93. doi:10.1021/acs.iecr.4c03453
61. Loachamin D, Casierra J, Calva V, Palma-Cando A, Ávila EE, Ricaurte M. Amine-Based Solvents and Additives to Improve the CO<sub>2</sub> Capture Processes: A Review. *ChemEngineering.* 2024 Dec 13;8(6):129. doi:10.3390/chemengineering8060129
62. Jiang X, Lin L, Rong Y, Li R, Jiang Q, Yang Y, et al. Boosting CO<sub>2</sub> electroreduction to formate via bismuth oxide clusters. *Nano Res.* 2023 Oct 9;16(10):12050–7. doi:10.1007/s12274-022-5073-0
63. Li L, Ozden A, Guo S, García de Arquer FP, Wang C, Zhang M, et al. Stable, active CO<sub>2</sub> reduction to formate via redox-modulated stabilization of active sites. *Nat Commun.* 2021 Sep 1;12(1):5223. doi:10.1038/s41467-021-25573-9
64. Rouf S, Greish YE, Van der Bruggen B, Al-Zuhair S. Enhancement of CO<sub>2</sub> hydrogenation to formate using formate dehydrogenase immobilized on UiO66 and its derivatives. *Green Synth Catal.* 2025 May;6(2):140–56. doi:10.1016/j.gresc.2024.09.005
65. Lee J, Kim SM, Jeon BW, Hwang HW, Poloniataki EG, Kang J, et al. Molar-scale formate production via enzymatic hydration of industrial off-gases. *Nature Chemical Engineering.* 2024 May 7;1(5):354–64. doi:10.1038/s44286-024-00063-z
66. Miyazaki M, Shibue M, Ogino K, Nakamura H, Maeda H. Enzymatic synthesis of pyruvic acid from acetaldehyde and carbon dioxide. *Chem Commun.* 2001;(18):1800–1. doi:10.1039/b104873m
67. Sajnani S, Memon MA, Memon SA, Kumar A, Mehvish D, Ameen S, et al. CO<sub>2</sub> to Methanol Conversion: A Bibliometric Analysis with Insights into Reaction Mechanisms, and Recent Advances in Catalytic Conversion. *Processes.* 2025 Jan 23;13(2):314. doi:10.3390/pr13020314
68. Wang D, Du Y, Liao Z, Hong X, Zhang S. Liquid-phase CO<sub>2</sub> hydrogenation to methanol synthesis: Solvent screening, process design and techno-economic evaluation. *J CO<sub>2</sub> Util.* 2024 Dec;90:102976. doi:10.1016/j.jcou.2024.102976
69. Fink AG, Lees EW, Gingras J, Madore E, Fradette S, Jaffer SA, et al. Electrolytic conversion of carbon capture solutions containing carbonic anhydrase. *J Inorg Biochem.* 2022 Jun;231:111782. doi:10.1016/j.jinorgbio.2022.111782
70. Villa R, Nieto S, Donaire A, Lozano P. Direct Biocatalytic Processes for CO<sub>2</sub> Capture as a Green Tool to Produce Value-Added Chemicals. *Molecules.* 2023 Jul 19;28(14):5520. doi:10.3390/molecules28145520
71. Sheldon RA, Brady D. Green Chemistry, Biocatalysis, and the Chemical Industry of the Future. *ChemSusChem.* 2022 May 6;15(9). doi:10.1002/cssc.202102628



72. Yuan L, Bonku EM, Yang ZH. Biocatalysis-driven CO<sub>2</sub> valorization: Innovations and sustainable strategies in conversion and utilization. *Carbon Capture Sci Technol*. 2025 Jun;15:100437. doi:10.1016/j.ccst.2025.100437
73. Ai L, Ng S, Ong W. A Prospective Life Cycle Assessment of Electrochemical CO<sub>2</sub> Reduction to Selective Formic Acid and Ethylene. *ChemSusChem*. 2022 Oct 10;15(19). doi:10.1002/cssc.202200857
74. Aldaco R, Butnar I, Margallo M, Laso J, Rumayor M, Dominguez-Ramos A, et al. Bringing value to the chemical industry from capture, storage and use of CO<sub>2</sub>: A dynamic LCA of formic acid production. *Sci Total Environ*. 2019 May;663:738–53. doi:10.1016/j.scitotenv.2019.01.395
75. Blazer SJ, Wang Y, Xu N, Zhou XD, Marchetti B. A systematic life cycle assessment of the electroconversion of carbon dioxide. *Sustain Energy Technol Assess*. 2024 Jan;61:103574. doi:10.1016/j.seta.2023.103574
76. Somoza-Tornos A, Guerra OJ, Crow AM, Smith WA, Hodge BM. Process modeling, techno-economic assessment, and life cycle assessment of the electrochemical reduction of CO<sub>2</sub>: a review. *iScience*. 2021 Jul;24(7):102813. doi:10.1016/j.isci.2021.102813
77. Kang D, Byun J, Han J. Electrochemical production of formic acid from carbon dioxide: A life cycle assessment study. *J Environ Chem Eng*. 2021 Oct;9(5):106130. doi:10.1016/j.jece.2021.106130
78. Sternberg A, Jens CM, Bardow A. Life cycle assessment of CO<sub>2</sub>-based C1-chemicals. *Green Chem*. 2017;19(9):2244–59. doi:10.1039/C6GC02852G
79. Badger N, Mattice D, Atwood M, Amini S. Life cycle assessment of formic acid synthesis utilizing CO<sub>2</sub> from direct air capture. *RSC Sustainability*. 2025;3(5):2404–21. doi:10.1039/D5SU00111K



## Data Availability Statement

View Article Online  
DOI: 10.1039/D6GC00387G

All datasets generated or analyzed during this study are available at <https://doi.org/10.34810/data2645>. Supplementary information: Experimental procedures for the co-immobilization of FDH and GlyDH enzymes, activity assays, protein content measurement, and HPLC analysis. Equations for the response time of the dissolved CO<sub>2</sub> sensor, its operating diagram, and the CO<sub>2</sub> mass balance equations. Scheme of the reaction mechanism for GC formation. Results of the determination of the response time of the dissolved CO<sub>2</sub> sensor, determination of the volumetric mass transfer coefficient ( $k_L a$ ) of CO<sub>2</sub> under different conditions, performances metrics of yields and productivity, pH monitoring, time-course of substrates and products, and monitoring of dissolved CO<sub>2</sub> concentrations and inlet/outlet CO<sub>2</sub> fractions during multi-enzymatic CO<sub>2</sub> reduction reactions.

